CrystEngComm

Cite this: *CrystEngComm*, 2012, **14**, 6441–6446

www.rsc.org/crystengcomm

PAPER

The unexpected but predictable tetrazole packing in flexible 1-benzyl-1*H*-tetrazole†

John Spencer,[ab] Hiren Patel,[a] John J. Deadman,[c] Rex A. Palmer,*[d] Louise Male,[ef] Simon J. Coles,[e] Ogaga G. Uzoh[g] and Sarah L. Price[g]

Received 12th June 2012, Accepted 3rd August 2012
DOI: 10.1039/c2ce25940k

The crystal structure of 1-benzyl-*1H*-tetrazole, $C_8H_8N_4$, was undertaken to study the geometry and intermolecular interactions of the (1-substituted) *1H*-tetrazole moiety. It crystallizes in the monoclinic space group $P2_1$ with unit cell dimensions a = 7.6843(5), b = 5.5794(4), c = 9.4459(7) Å, β = 100.949(4)°, V = 397.61(5) Å^3, Z = 2, density (calculated) = 1.338 gcm^{-3}. The packing of the molecules in the crystal structure is dominated by a number of weak intermolecular hydrogen bonds of the type CH···N and CH···C. This results in segregated infinite S-shaped layers of phenyl and tetrazole rings where each tetrazole ring is coordinated by six others. There are no π···π interactions. A group developing crystal structure prediction methods for highly flexible molecules was challenged to predict this Z′ = 1 crystal structure from the chemical diagram. The experimental structure was found, having essentially the same lattice energy (ΔE_{latt} ~0.1 kJmol^{-1}) as the most stable computationally generated structure, which had the expected π···π interaction and no segregation of tetrazole rings. The successful crystal structure prediction confirms that the intra and intermolecular interactions of the tetrazole group can be adequately represented by single molecule *ab initio*-based methods, which represent the electrostatic effects of the lone pairs and π electron density. The predicted structure provided a starting model, which was easily refined in SHELXL-97, providing indisputable proof that it is an accurate reproduction of the crystal structure.

Introduction

The 5-substituted *1H*-tetrazole motif (Fig. 1a) has been frequently mentioned in the drug discovery literature as a bioisostere for the carboxylic acid group, due to their similar pK_a values, shape and steric interactions. A recent study[1] using crystal structures in the Cambridge Structural Database (CSD),[2] shows that both the *1H*-tetrazole/COOH and tetrazolate/carboxylate isosteric pairs exhibit very similar hydrogen bonding environments and energies. In contrast, a short review,[3] which discusses data on drugs containing tetrazole, a synthetic moiety that is not known to occur in nature, shows that the 1-substituted *1H*-tetrazole (Fig. 1b) has not yet been widely used in the design of pharmaceutical products. The best known are derivatives of β-lactam antibiotics and optically active tetrazole-based antifungal preparations of the azole type, such as TAK-456 (Fig. 1c).[4,5] The latter exhibits potent activity against *Candida*, *Cryptococcus* and *Aspergillus* when administered perorally. An improved water-soluble form of TAK-457 was developed from TAK-456 (Fig. 1c).[4,5]

Since the review[3] there has been a marked increase in the number of crystal structures in the CSD containing the 1-substituted C–H version, with 32 such tetrazole molecules in version 5.33 March 2012, but this list includes only one drug-like compound (refcode BEGRIP)[4] a derivative of TAK456 (Fig. 1c). The steric differences between the 1 and 5-substituted *1H*-tetrazoles may be small (Fig. 1a and b), but the intermolecular interactions are very different, as the N–H group is a classic hydrogen bond donor, but the C–H group is much less polar. The review[3] depicts the distribution of bonds in the tetrazole ring without reference to any crystal structural data. Hence, the X-ray structure of 1-benzyl-*1H*-tetrazole, $C_8H_8N_4$, (Fig. 2), was undertaken in order to consolidate data on the geometry and chemical nature of the bonds in the *1H*-tetrazole moiety. It was

[a]*School of Science, University of Greenwich, Medway Campus, Central Avenue, Chatham Maritime, Kent ME4 4TB, United Kingdom*
[b]*Department of Chemistry, School of Life Sciences, University of Sussex, Falmer, Brighton, East Sussex, BN1 9QJ, United Kingdom*
[c]*JDJ Biosciences, 576 Swan Street, Melbourne, 3121, Australia*
[d]*School of Crystallography, Birkbeck College, University of London, Malet Street, London, WC1E 7HX, United Kingdom. E-mail: rex.palmer@btinternet.com*
[e]*National X-ray Crystallography Unit Department of Chemistry, University of Southampton, Southampton, SO17 1BJ, United Kingdom*
[f]*School of Chemistry, University of Birmingham, Edgbaston, Birmingham, B15 2TT, United Kingdom*
[g]*Department of Chemistry, University College London, 20 Gordon Street, London, WC1H 0AJ, United Kingdom*

† Electronic supplementary information (ESI) available: Crystallographic data tables, the conformational energy grid used in the search, table of low energy computed crystal structures, further comparisons with other tetrazole structures. CCDC reference number 804779. For ESI and crystallographic data in CIF or other electronic format see DOI: 10.1039/c2ce25940k

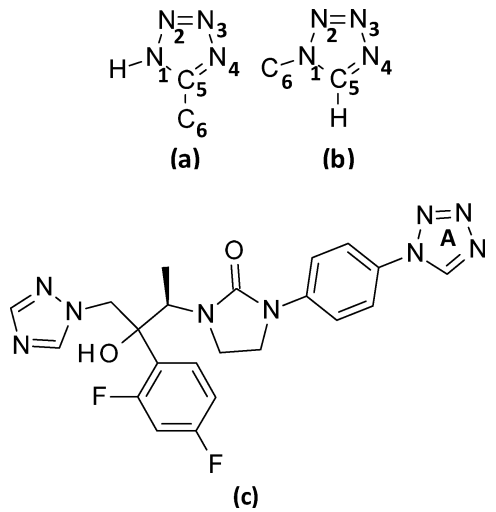

Fig. 1 The *1H*-tetrazole moiety (a) 5-substituted *1H*-tetrazole (b) 1-substituted *1H*-tetrazole and (c) the antifungal TAK-456,1-[(1*R*,2*R*)-2-(2,4-difluorophenyl)-2-hydroxy-1-methyl-3-(*1H*-1,2,4-triazol-1-yl) propyl]-3-[4-(*1H*-1-tetrazolyl)phenyl]-2-imidazolidinone an example of an active compound having a *1H*-tetrazole group (A).

also seen as a test of the competing intermolecular interactions between this tetrazole and a phenyl ring, in the expectation that some form of π···π stacking of the two aromatic groups might be the dominant packing motif.

The expected mode of packing was not realized and instead an unusual mode of packing was observed. Consequently, it was decided to carry out a completely independent blind crystal structure prediction of 1-benzyl-*1H*-tetrazole. This would provide a stringent test of the ability to predict the crystal structure of a molecule with sufficient conformational flexibility to adopt a wide range of molecular shapes, and that contains an unusual functional group with a different electronic structure from those used in developing the CSP methodology.

Experimental

1-Benzyl-*1H*-tetrazole, $C_8H_8N_4$ was synthesised according to the literature method on a *ca.* 50 mmol scale from benzylamine, sodium azide and triethylformate. Its spectroscopic and analytical data were consistent with those of the literature.[6] It was crystallized from dichloromethane/hexane by the vapour diffusion method.

Data collection

A colourless crystal fragment of dimensions 0.09 × 0.03 × 0.02 mm^3 was mounted on a glass fibre and flash frozen to 120 K. Intensities were collected, using monochromated Mo-Kα radiation, λ = 0.71073 Å, on a Bruker-Nonius APEX II CCD camera, employing φ and ω scans to cover an asymmetric unit. Programs used were: unit cell determination with the program DirAx;[7] data collection controlled by Collect;[8] data reduction and cell refinement using the program Denzo;[9] an absorption correction was made with SORTAV.[10,11] An Oxford Cryosystems Cryostreams 700,[12] enabled the data to be collected at 120 K. The crystals are monoclinic space group $P2_1$ with unit cell dimensions a = 7.6843(5), b = 5.5794(4), c = 9.4459(7) Å, β = 100.949(4)°, V = 397.61(5) $Å^3$, Z = 2, density (calculated) = 1.338 gcm^{-3}, linear absorption coefficient = 0.088 mm^{-1}. The crystal structure determination was carried out with Mo-Kα X-ray data measured at 120(2) K. In total 5629 integrated reflections were collected, reducing to a data set of 977 [R_{int} = 0.0625], and completeness of data to θ = 27.45° of 98.4%. The resolution range was 6.49 to 0.771 Å. There was no significant variation in intensity during the course of data collection.

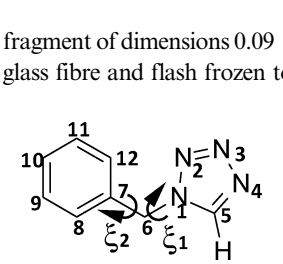

Fig. 2 1-Benzyl-*1H*-tetrazole showing the tetrazole ring bond distribution determined from the current analysis and the torsion angles ξ_1 = C(7)–C(6)–N(1)–C(5) and ξ_2 = C(12)–C(7)–C(6)–N(1) which were allowed to vary in the CSP search.

X-ray structure analysis

The crystal structure was solved by Direct Methods and refined using SHELXL-97[13,14] implemented in the WinGX system of programs.[15] In the final refinement cycles Friedel pairs were merged because in previous cycles the Flack parameter[16] had failed to resolve the absolute space group configuration. The molecule does not contain any anomalous scatterers or asymmetric centres so this result has little or no consequence. Non-hydrogen atoms were refined anisotropically by full-matrix least squares methods. Benzyl and CH_2 protons were set geometrically and refined in riding mode. H(5) on C(5) in the tetrazole ring was located on an electron density difference map and freely refined isotropically. Geometrical calculations including characterization of intermolecular CH···N and CH···H contacts were made with the program PARST[17] as implemented in WinGX. In the final refinement cycle there were 977 data to 113 parameters, resulting in a final goodness-of-fit on F^2 of 1.259. Final R indices for [$I > 2\sigma(I)$] were R_1 = 0.0426, wR_2 = 0.0753 and R indices (all data) R_1 = 0.0636, wR_2 = 0.0827. The largest and smallest difference electron density regions were +0.186 and −0.207 e$Å^{-3}$ respectively. Crystal data are summarized in ESI, Table S1†.

Crystal structure prediction

Those working on this independent prediction study were provided only with the chemical diagram of the molecule and were informed that the crystal structure had one molecule per asymmetric unit. Initially the modelling study investigated possible steric hindrance to rotation about the two torsion angles ξ_1 and ξ_2 (Fig. 2 and ESI, Fig. S1†), which indicated a high degree of flexibility in the molecule. This degree of flexibility, where a wide range of very different molecular shapes are possible, has to be taken into account from the beginning of the search, a significant change to the approach that can be used for nearly rigid molecules.[18–20] The methodology used here for the prediction of crystal structures of flexible molecules was that developed and successfully used[21] for a pharmaceutical-like molecule, with 7 torsion angles linking four aromatic rings and a peptide group, in the fifth blind test of crystal structure prediction.[22]

The search using the program CrystalPredictor[23] covering the 59 most commonly occurring space groups, generated about 170 000 structures. The lattice energy, $E_{latt} = U_{inter} + \Delta E_{intra}$, where U_{inter} is the intermolecular packing energy and ΔE_{intra} is the energy penalty for changing the conformation of the molecule, was minimised by varying the cell parameters and torsion angles ξ_1 and ξ_2. At this stage the lattice energy was crudely calculated by using a grid of *ab initio* calculations for ΔE_{intra}, and an atomic point charge model and empirical repulsion-dispersion model for U_{inter}. Minimising this lattice energy reduced the search to approximately 44 000 unique structures, which were labelled by their energy ordering with this atomic-charge-model based intermolecular potential.

The model for the electrostatic interactions and conformational energy was then improved. For each of the lowest 10 000 crystal structures, the energy of the molecule and its charge distribution were calculated at the PBE0/6-31G(d,p) level of theory, using GAUSSIAN,[24] to provide a better estimate of ΔE_{intra}, and a more accurate representation of the charge density in terms of a distributed multipole model[25] using GDMA.[26] This was combined with an atom-atom exp-*6* repulsion-dispersion potential using parameters that had been fitted to azahydrocarbons[27] and polar crystal structures,[28] which were assumed transferable to this tetrazole. The crystal structure was lattice energy minimised, with the molecule held rigid using DMACRYS.[29] The 100 most stable structures were then further refined by allowing the molecular conformation to adjust more accurately to the intermolecular forces using the program CrystalOptimizer[30,31] to combine GAUSSIAN[24] calculations on the molecular conformations and DMACRYS[29] optimisations of the crystal structure. Finally, the effect of the crystal environment on the conformational energies ΔE_{intra} and charge density was estimated by calculating the conformational energy and charge distribution in a polarizable continuum, with $\varepsilon = 3$, a value typical of organic molecules,[32] using the Polarizable Continuum Model (PCM)[33] as implemented in GAUSSIAN[24] at PBE0/6-31+G(d) level of theory.

Results and discussion

Molecular geometry

Overall the benzyl and tetrazole rings are essentially planar, including the H atom on the CH group belonging to the 5-membered tetrazole ring. The individual rings are also each coplanar with the inter-ring link C atom. The dihedral angle between the two rings is 68.52(5)° (Fig. 3). The N–N bonds are of three different types, consistent with Fig. 2: N(1)–N(2) = 1.343(2) Å is typically of a diazene; N(2)–N(3) = 1.301(2) Å is longer than a typical N=N bond[36] but shorter than a typical aromatic bond; N(3)–N(4) = 1.368(2) Å is also largely aromatic in character.[36] The two C–N bonds have different characteristics: C(5)–N(4) = 1.314(2) Å is a double bond; C(5)–N(1) = 1.336(2) Å is typically aromatic.[36] The experimental bond lengths are also typical of those in the other crystal structures containing the 1-substituted *1H*-tetrazole group (Fig. 4). There are some significant differences ($\leqslant$ 0.02 Å) between the *ab initio* computed values and experimental bond lengths, but both are within the observed ranges. The variations in tetrazole bond angles (ESI, Fig. S4†) are consistent with the bond length variations for this moiety,

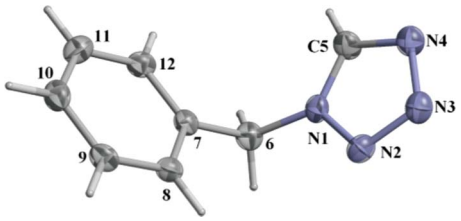

Fig. 3 1-Benzyl-*1H*-tetrazole showing thermal ellipsoids at 50% probability. ξ_1 = C(7)–C(6)–N(1)–C(5) = −89.8(3)° and ξ_2 = C(12)–C(7)–C(6)–N(1) = 98.5(3)°. Drawn with ORTEP[34] and RASTER3D.[35]

which is always close to planar. The external torsions angles, ξ_1 and ξ_2 exhibit a wide range of values (ESI, Fig. S4†), which is consistent with the large range of low energy conformations (ESI, Fig. S1†) despite the range of functional groups bonded to C(6).

Crystal packing: weak hydrogen bonding

The mode of packing of the molecules in this crystal structure is unusual. A molecule such as 1-benzyl-*1H*-tetrazole, based on linked delocalized rings, might be expected to form crystal

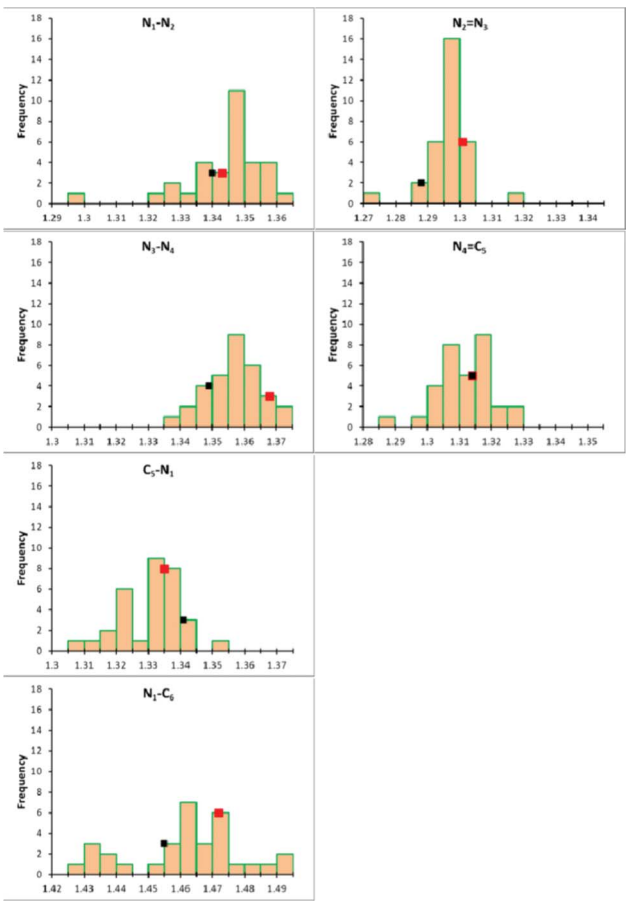

Fig. 4 Histograms showing the bond length distributions of 32 1-susbtituted *1H*-tetrazole rings in the CSD. The experimental bondlength in1-benzyl-*1H*-tetrazole is denoted by the red square, while the *ab initio* bondlength in the corresponding calculated structure #2BT_23 is denoted by the black square.

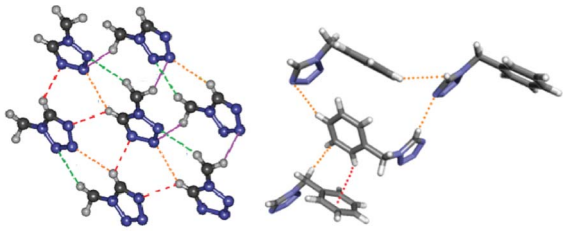

(a) (b)

Fig. 5 1-Benzyl-*1H*-tetrazole crystal structure: (a) partial view of the crystal packing showing close CH···N contacts between a central tetrazole and six surrounding tetrazoles (see also ESI, Table S3†); (b) partial view showing CH···N, CH···C and CH···π contacts.

structures involving π···π bonding (ring stacking). However, no such interactions occur in the present structure (Fig. 5). Instead, the structure is held together through a large number of weak intermolecular hydrogen bonds:[37,38] 12 of these are of the type CH···N; and 3 are of the weaker type CH···C (ESI, Table S3†) involving atoms in the phenyl ring.

This results in a structure composed of infinite S-shaped layers, producing a sequence of benzyl and tetrazole layers (Fig. 6). An unexpected feature of the packing is the formation of tetrazole clusters (Fig. 5a), each having a central tetrazole ring coordinated by six other tetrazoles.

Crystal energy landscape

The two most stable crystal structures on the crystal energy landscape (Fig. 7) are separated by less than 0.1 kJ mol^{-1} but are very different from each other. One of these structures, labelled #2BT_23, is in the same space group, $P2_1$, as determined experimentally and has very similar unit cell dimensions (ESI, Table S4†). This computed structure gives an excellent overlay with the experimental structure using the COMPACK[39] facility as implemented in MERCURY,[40] with a root mean square difference in the positions of the non-hydrogen atoms in a 15 molecule cluster being only 0.148 Å (Fig. 8). #2BT_23 provided a starting model easily refined in SHELXL-97, which is further proof that it is a genuine reproduction of the crystal structure.

The structure corresponding to the global minimum in lattice energy, #1BT_120 (ESI, Table S4†), is in space group $P2_1/c$ and

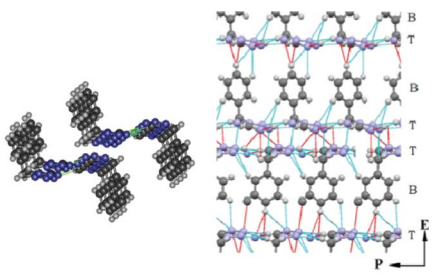

(a) (b)

Fig. 6 1-Benzyl-*1H*-tetrazole crystal structure: (a) View of the infinite S-shaped layers held together by weak CH···N and CH···C hydrogen bonds; (b) Partial view of the layer structure showing alternative B(benzyl) and T(tetrazole) layers, and the repeating layer sequence [BTBT|TBTB].

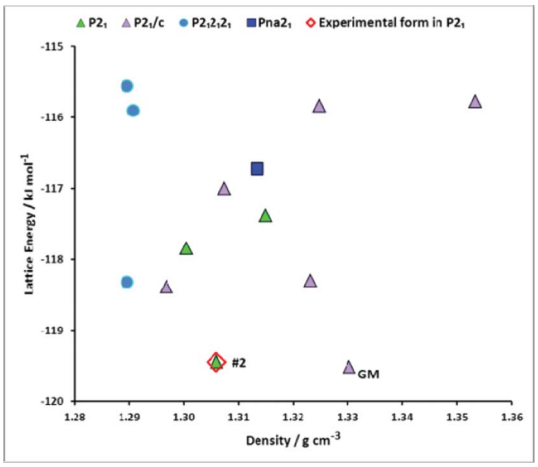

Fig. 7 Crystal energy landscape of 1-benzyl-*1H*-tetrazole. Each point represents a crystal structure that is a lattice energy minimum with the final PCM model. The structure that matches the experimental crystal structure, #2BT_23 is labelled with its energy rank #2. The global minimum structure #1BT_120 is labelled GM.

presents a very different spatial arrangement as shown in Fig. 9. This structure also has dominant weak hydrogen bonds: 8 of type CH···N; and 1 CH···C. There is also one weak π···π, benzyl···benzyl interaction (Fig. 9). Thermodynamically, this structure could be a polymorph of 1-benzyl-*1H*-tetrazole.

Examining this lowest energy calculated structure and the 32 1-substituted *1H*-tetrazole structures in the CSD show that none have the tetrazole cluster seen in the experimental structure. However, there is some form of tetrazole layer in #1BT_120 and the experimental structures DOKQIE, EKAJOQ, QALPAV, QALPOJ, QALPUP and REVMOV, all of which have the tetrazole bonded to a sp^3 carbon and are tetrazole hydrocarbons (except QALPAV, which also contains an iodine atom). Hence, there is no strong driving force for the tetrazole cluster, but a layer structure does seem quite favourable, in cases where there are no competing strong interactions.

The successful prediction of a crystal structure is usually a severe test of the accuracy of the models used to calculate the

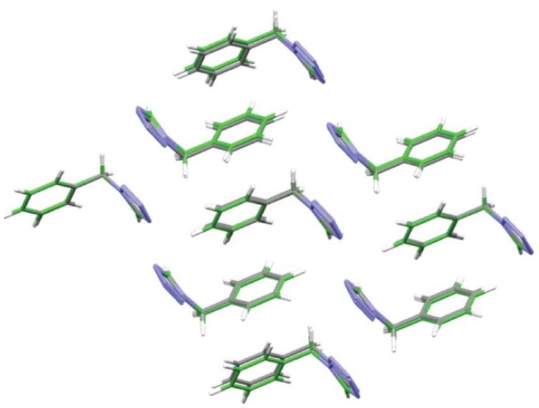

Fig. 8 Overlay 15 molecules of the experimental (atomic colours) and the second most stable computed structure, #2BT_23 (green). The direction of view obscures some of the molecules.

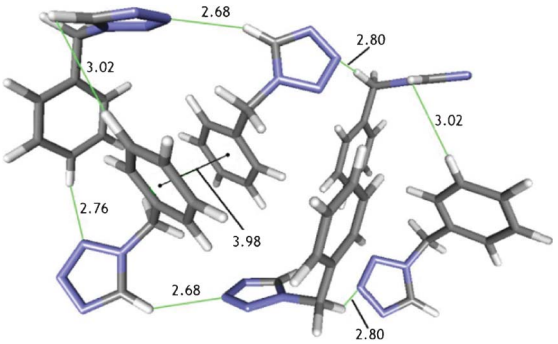

Fig. 9 The structure corresponding to the global minimum in lattice energy, #1BT_23 showing the dominant weak hydrogen bonds (Å): 8 of type CH···N; and 1 CH···C and the weak π···π interaction (benzyl···benzyl).

lattice energy,[22] and this success demonstrates that the approach used was able to balance the competing intramolecular and intermolecular interactions between the tetrazole and phenyl groups, without any specific reference to experimental data on *1H*-tetrazoles. The test molecule has a wide range of low energy conformations (ESI, Fig. S1†) and the molecule adopts a conformation that is within a few kJ mol^{-1} of the most stable isolated molecule conformation in most of the low energy crystal structures (ESI, Table S4†). The key to the successful prediction was the use of a conformation dependent distributed multipole representation of the electrostatic forces, as this improvement on an atomic charge model (ESI, Fig. S2†) caused by far the most substantial reranking of the hypothetical crystal structures by lattice energy (contrast Fig. 7, ESI, Table S4 and Fig. S2†). The structure that was lowest in energy after the CrystalPredictor search was 9 kJ mol^{-1} above the experimental structure in the final lattice energy model and had markedly fewer close contacts than the experimental structure (#2BT_23).

The successful prediction of the crystal packing preferences of the tetrazole group, and the failure with a conventional point charge electrostatic model, has considerable implications for other studies that rely on modelling the intermolecular interactions of 1-substituted *1H*-tetrazoles. This study illustrates the use of crystal structures to assess the reliabilities of force-fields.[41] It also provides hope that the use of multipolar electrostatic models (as being implemented in the second generation force-fields such as AMOEBA[42]) with careful evaluation of the accuracy of the intramolecular forces, will provide a route forward to greater reliability for computer-aided drug design with uncommon ligands.

Conclusions

The X-ray crystal structure of 1-benzyl-*1H*-tetrazole shows an unusual crystal packing with segregated layers of phenyl and tetrazole interactions, tetrazole clusters and no π···π interactions. This packing was predicted from the chemical diagram by a model that accurately modelled the electrostatic forces arising from molecular charge density, including the anisotropic forces from the lone pair and π electrons, but otherwise had not been tailored to the tetrazole···tetrazole interactions. The successful prediction of the experimental structure as one of the two distinct most stable structures shows that the unusual layers do present an optimal compromise between the many different weak hydrogen bonds and other intermolecular interactions. Conversely, it also shows that the level of computational chemistry modelling used is suitable for modelling the molecular recognition of this functional group, which could become increasingly useful in pharmaceutical design.

Acknowledgements

We thank Avexa for funding the PhD degree of Hiren Patel. OGU is financially supported by CCDC and EPSRC EP/G036675/1 (M3S Centre for Doctoral Training). The CPOSS project CSP infrastructure is EPSRC funded under EP/F03573X/1.

References

1 F. H. Allen, C. R. Groom, J. W. Liebeschuetz, D. A. Bardwell, T. S. G. Olsson and P. A. Wood, *J. Chem. Inf. Model.*, 2012, **52**, 857–866.
2 F. H. Allen, *Acta Crystallogr., Sect. B: Struct. Sci.*, 2002, **58**, 380–388.
3 L. Myznikov, A. Hrabalek and G. Koldobskii, *Chem. Heterocycl. Compd.*, 2007, **43**, 1–9.
4 T. Ichikawa, M. Yamada, M. Yamaguchi, T. Kitazaki, Y. Matsushita, K. Higashikawa and K. Itoh, *Chem. Pharm. Bull.*, 2001, **49**, 1110–1119.
5 T. Ichikawa, T. Kitazaki, Y. Matsushita, H. Hosono, M. Yamada, M. Mizuno and K. Itoh, *Chem. Pharm. Bull.*, 2000, **48**, 1947–1953.
6 Y. Satoh and N. Marcopulos, *Tetrahedron Lett.*, 1995, **36**, 1759–1762.
7 A. Duisenberg, *J. Appl. Crystallogr.*, 1992, **25**, 92–96.
8 R. Hooft, *COLLECT: Data Collection Software Nonius BV*, Delft, The Netherlands, 1998.
9 Z. Otwinowski and W. Minor, in *Methods in Enzymology Macromolecular Crystallography Part A*, ed. W. Carter Charles, Academic Press, **Volume 276**, 1997, pp 307–326.
10 R. Blessing, *Acta Crystallogr., Sect. A: Found. Crystallogr.*, 1995, **51**, 33–38.
11 R. Blessing, *J. Appl. Crystallogr.*, 1997, **30**, 421–426.
12 J. Cosier and A. M. Glazer, *J. Appl. Crystallogr.*, 1986, **19**, 105–107.
13 G. M. Sheldrick, *SHELXL97 University of Göttingen Göttingen*, Germany, 1997.
14 G. M. Sheldrick, *Acta Crystallogr., Sect. A: Found. Crystallogr.*, 2007, **64**, 112–122.
15 L. Farrugia, *J. Appl. Crystallogr.*, 1999, **32**, 837–838.
16 H. Flack, *Acta Crystallogr., Sect. A: Found. Crystallogr.*, 1983, **39**, 876–881.
17 M. Nardelli, *J. Appl. Crystallogr.*, 1995, **28**, 659.
18 B. S. Potter, R. A. Palmer, R. Withnall, B. Z. Chowdhry and S. L. Price, *J. Mol. Struct.*, 1999, **485–486**, 349–361.
19 H. Nowell, C. S. Frampton, J. Waite and S. L. Price, *Acta Crystallogr., Sect. B: Struct. Sci.*, 2006, **62**, 642–650.
20 E. D'Oria, P. G. Karamertzanis and S. L. Price, *Cryst. Growth Des.*, 2010, **10**, 1749–1756.
21 A. V. Kazantsev, P. G. Karamertzanis, C. S. Adjiman, C. C. Pantelides, S. L. Price, P. T. Galek, G. M. Day and A. J. Cruz-Cabeza, *Int. J. Pharm.*, 2011, **418**, 168–178.
22 D. A. Bardwell, C. S. Adjiman, Y. A. Arnautova, E. Bartashevich, S. X. Boerrigter, D. E. Braun, A. J. Cruz-Cabeza, G. M. Day, R. G. la Valle, G. R. Desiraju, B. P. van Eijck, J. C. Facelli, M. B. Ferraro, D. Grillo, M. Habgood, D. W. Hofmann, F. Hofmann, K. Jose, V. P. G. Karamertzanis, A. V. Kazantsev, J. Kendrick, L. N. Kuleshova, F. J. Leusen, A. V. Maleev, A. J. Misquitta, S. Mohamed, R. J. Needs, M. A. Neumann, D. Nikylov, A. M. Orendt, R. Pal, C. C. Pantelides, C. J. Pickard, L. S. Price, S. L. Price, H. A. Scheraga, J. van de Streek, T. S. Thakur, S. Tiwari, E. Venuti and I. K. Zhitkov, *Acta Crystallogr., Sect. B: Struct. Sci.*, 2011, **67**, 535–551.
23 P. G. Karamertzanis and C. C. Pantelides, *Mol. Phys.*, 2007, **105**, 273–291.

24 M. J. Frisch, G. W. Trucks, H. B. Schlegel, G. E. Scuseria, M. A. Robb, J. R. Cheeseman, J. Montgomery, T. Vreven, K. N. Kudin, J. C. Burant, J. M. Millam, S. S. Iyengar, J. Tomasi, V. Barone, B. Mennucci, M. Cossi, G. Scalmani, N. Rega, G. A. Petersson, H. Nakatsuji, M. Hada, M. Ehara, K. Toyota, R. Fukuda, J. Hasegawa, M. Ishida, T. Nakajima, Y. Honda, O. Kitao, H. Nakai, M. Klene, X. Li, J. E. Knox, H. P. Hratchian, J. B. Cross, V. Bakken, C. Adamo, J. Jaramillo, R. Gomperts, R. E. Stratmann, O. Yazyev, A. J. Austin, R. Cammi, C. Pomelli, J. Ochterski, P. Y. Ayala, K. Morokuma, G. A. Voth, P. Salvador, J. J. Dannenberg, V. G. Zakrzewski, S. Dapprich, A. D. Daniels, M. C. Strain, O. Farkas, D. K. Malick, A. D. Rabuck, K. Raghavachari, J. B. Foresman, J. V. Ortiz, Q. Cui, A. G. Baboul, S. Clifford, J. Cioslowski, B. B. Stefanov, G. Liu, A. Liashenko, P. Piskorz, I. Komaromi, R. L. Martin, D. J. Fox, T. Keith, M. A. Al Laham, C. Y. Peng, A. Nanayakkara, M. Challacombe, P. M. W. Gill, B. Johnson, W. Chen, M. W. Wong, C. Gonzalez and J. A. Pople, Gaussian 03 Gaussian Inc. Wallingford CT, 2004.
25 A. J. Stone, *J. Chem. Theory Comput.*, 2005, **1**, 1128–1132.
26 A. J. Stone, *GDMA: A Program for Performing Distributed Multipole Analysis of Wave Functions Calculated Using the Gaussian Program System [2.2]*. University of Cambridge, Cambridge, United Kingdom, 2010.
27 D. E. Williams and S. R. Cox, *Acta Crystallogr., Sect. B: Struct. Sci.*, 1984, **40**, 404–417.
28 D. S. Coombes, S. L. Price, D. J. Willock and M. Leslie, *J. Phys. Chem.*, 1996, **100**, 7352–7360.
29 S. L. Price, M. Leslie, G. W. A. Welch, M. Habgood, L. S. Price, P. G. Karamertzanis and G. M. Day, *Phys. Chem. Chem. Phys.*, 2010, **12**, 8478–8490.
30 A. V. Kazantsev, P. G. Karamertzanis, C. S. Adjiman and C. C. Pantelides, *J. Chem. Theory Comput.*, 2011, **7**, 1998–2016.
31 A. V. Kazantsev, P. G. Karamertzanis, C. S. Adjiman and C. C. Pantelides, in *Molecular System Engineering*, C. S. Adjiman and A. Galindo, WILEY-VCH Verlag GmbH & Co., Weinheim, 2010 Chapter 1, pp. 1–42.
32 T. G. Cooper, K. E. Hejczyk, W. Jones and G. M. Day, *J. Chem. Theory Comput.*, 2008, **4**, 1795–1805.
33 M. Cossi, G. Scalmani, N. Rega and V. Barone, *J. Chem. Phys.*, 2002, **117**, 43–45.
34 C. Barnes, *J. Appl. Crystallogr.*, 1997, **30**, 568.
35 E. A. Merritt and D. J. Bacon, in *Methods in Enzymology Macromolecular Crystallography Part B*, ed. W. Carter Charles, Jr., Academic Press, **Volume 277**, 1997, pp. 505–524.
36 M. F. C. Ladd and R. A. Palmer, *Structure Determination by X-Ray Crystallography*, Springer, 2003.
37 G. R. Desiraju, *Acc. Chem. Res.*, 2002, **35**, 565–573.
38 W. A. Herrebout and M. A. Suhm, *Phys. Chem. Chem. Phys.*, 2011, **13**, 13858.
39 J. A. Chisholm and S. Motherwell, *J. Appl. Crystallogr.*, 2005, **38**, 228–231.
40 C. F. Macrae, P. R. Edgington, P. McCabe, E. Pidcock, G. P. Shields, R. Taylor, M. Towler and J. van de Streek, *J. Appl. Crystallogr.*, 2006, **39**, 453–457.
41 T. R. Stouch, *J. Comput.-Aided Mol. Des.*, 2012, **26**, 1.
42 J. W. Ponder, C. J. Wu, P. Y. Ren, V. S. Pande, J. D. Chodera, M. J. Schnieders, I. Haque, D. L. Mobley, D. S. Lambrecht, R. A. DiStasio, M. Head-Gordon, G. N. I. Clark, M. E. Johnson and T. Head-Gordon, *J. Phys. Chem. B*, 2010, **114**, 2549–2564.

